A STUDY OF THE MAGNETO-KERR AND OTHER EFFECTS AT A PLASMA SURFACE

By L. C. Robinson*

[*Manuscript received June* 30, 1966]

Summary

The role of microwave reflection observations and particularly the magneto-microwave Kerr effect in the study of plasma surface phenomena is discussed. The method makes possible the absolute measurement of high electron surface densities in a density region not readily accessible to other experimental techniques, and it gives an indication of the collision frequency for momentum transfer.

To facilitate the interpretation of measurements in terms of plasma parameters, curves are computed for a step-function plasma profile giving the dependence of reflection on surface electron density and collision frequency over a wide range of magnetic induction fields and microwave frequencies. The results are directly applicable to the three microwave frequencies commonly used in plasma physics research, namely 10, 35, and 120 Gc/s. From an analysis of the dependence of the magnitudes and phases of the reflection coefficients of circularly and linearly polarized incident waves the relative value of the various possible waves and combinations of waves for plasma diagnostic experiments is assessed.

The effects of variations from a step-function plasma density profile are considered. Polynomial expressions are derived giving the factor by which the amplitudes and phases of the reflection coefficients are modified when the density rises exponentially to a plateau level, and this factor is computed for steep gradients.

I. Introduction

During the past few years an active interest in the study of plasma surface phenomena by microwave reflection methods has been developing in a number of laboratories throughout the world. For suitably abrupt surfaces the reflection coefficient is sensitive to electron densities some orders of magnitude in excess of those normally accessible to microwave interferometry and can be used as a diagnostic tool to observe densities in the range 10^{12}–10^{16} cm^{-3}.

Much of the work has stemmed from Takeda in Japan (Takeda and Roux 1961; Tsukishima and Takeda 1962; Takeda and Tsukishima 1963), and this method has been extended in the U.S.A. (McLane *et al.* 1964) and Germany (Hermansdorfer 1965). The experimental technique of these workers has involved the use of waveguides terminated with dielectric windows which either enclose plasma or penetrate the surface or body of a large plasma; the amplitude and phase of the reflection are separately measured, the latter by waveguide probe techniques. These studies have been performed with conventional gas discharges and with shock tube and linear Z-pinch plasmas. They have mainly involved isotropic wave–plasma interactions.

In Sydney we have explored the possibilities of microwave reflections since 1962 but along independent and somewhat different lines. Our experiments have

* Wills Plasma Physics Department, School of Physics, University of Sydney.

been performed with an anisotropic surface of a shock-produced plasma and with free-space waves (Robinson 1965; Brand, Chung, and Robinson 1966). We have studied a plasma surface oriented at right angles to an applied magnetic induction field. A horn antenna some distance outside the plasma boundary has been used to radiate the microwaves at normal incidence and collect them after reflection. Rather than observe the phase and amplitude separately we have monitored and compared with theoretical predictions the total power reflection. Like those of the overseas workers, our initial observations were of the reflected-wave component with the same linear polarization as the incident wave, but more recently we have studied the component polarized orthogonally to this and have detected the magneto-microwave Kerr effect at a plasma surface (Robinson 1966).

In the present paper we calculate the reflection of waves that are right-hand circularly polarized (RHCP), left-hand circularly polarized (LHCP), and linearly polarized, incident normally on a plasma surface oriented at right angles to an applied magnetic induction field. From the behaviour of these various reflection coefficients as a function of electron density, collision frequency, magnetic induction field, and microwave frequency, we assess the relative values of these various waves for surface observations. We calculate the two orthogonal linearly polarized reflected components of an incident linearly polarized wave and give curves from which electron density and collision frequency in the plasma surface can be deduced. Our calculations are carried out for a step-function vacuum–plasma boundary, but a factor is calculated giving the effect of an exponential plasma-density profile.

II. Theory

In considering reflection at a step function of plasma density it is convenient to calculate separately the reflection of RHCP and LHCP waves. The coordinates rotating with these wave vectors are the principal coordinates, in which the complex effective dielectric constant is a diagonalized tensor. The rotating field vectors "see" a medium with a scalar effective complex refractive index, to which the boundary conditions readily relate the reflection coefficient (Robinson 1965).

We suppose waves of the form $\exp \mathrm{j}(\omega t - k_0 z)$ to be travelling in free space and at normal incidence towards the plasma surface. There is a magnetic field parallel to the z direction. From the linearized Boltzmann equation the components of the tensor dielectric constant can be shown to be (Stix 1962)

$$\left.\begin{aligned}
\epsilon_{\mathrm{R}} &= 1+\frac{\omega_{\mathrm{p}}^2}{\omega}\left[\frac{(\omega+\omega_{\mathrm{c}})(\nu^2+\omega_{\mathrm{c}}^2-\omega^2)-2\nu^2\omega-\mathrm{j}\nu\{\nu^2+\omega_{\mathrm{c}}^2-\omega^2+2\omega(\omega+\omega_{\mathrm{c}})\}}{(\nu^2+\omega_{\mathrm{c}}^2-\omega^2)^2+4\omega^2\nu^2}\right], \\
\epsilon_{\mathrm{L}} &= 1+\frac{\omega_{\mathrm{p}}^2}{\omega}\left[\frac{(\omega-\omega_{\mathrm{c}})(\nu^2+\omega_{\mathrm{c}}^2-\omega^2)-2\nu^2\omega-\mathrm{j}\nu\{\nu^2+\omega_{\mathrm{c}}^2-\omega^2+2\omega(\omega-\omega_{\mathrm{c}})\}}{(\nu^2+\omega_{\mathrm{c}}^2-\omega^2)^2+4\omega^2\nu^2}\right]
\end{aligned}\right\} \tag{1}$$

for the RHCP and LHCP waves respectively (throughout this paper the subscripts R and L denote the RHCP and LHCP waves; however, when we omit subscripts it is to be understood that the expressions apply to both the RHCP and LHCP waves, provided the appropriate expressions are substituted from such equations as (1)).

If we write the complex dielectric constant in the form

$$\epsilon = a - jb, \tag{2}$$

then the amplitude $|r|$ and the phase change at reflection θ of the reflection coefficient

$$r \equiv |r|\,e^{j\theta} = \frac{1-\epsilon^{\frac{1}{2}}}{1+\epsilon^{\frac{1}{2}}}$$

take the forms

$$|r| = \frac{\{(1-a)^2+b^2\}^{\frac{1}{2}}}{1+\{a^2+b^2\}^{\frac{1}{2}}+\sqrt{2}\{a+(a^2+b^2)^{\frac{1}{2}}\}^{\frac{1}{2}}}, \tag{3}$$

$$\theta = \tan^{-1}\left[\frac{\sqrt{2}\{(a^2+b^2)^{\frac{1}{2}}-a\}^{\frac{1}{2}}}{1-(a^2+b^2)^{\frac{1}{2}}}\right] \tag{4}$$

when $a > 0$. When $a < 0$,

$$|r| = \frac{1-\sqrt{2}\{(|a|^2+b^2)^{\frac{1}{2}}-|a|\}^{\frac{1}{2}}+(|a|^2+b^2)^{\frac{1}{2}}}{1+\sqrt{2}\{(|a|^2+b^2)^{\frac{1}{2}}-|a|\}^{\frac{1}{2}}+(|a|^2+b^2)^{\frac{1}{2}}}, \tag{5}$$

$$\theta = \tan^{-1}\left[\frac{\sqrt{2}\{(|a|^2+b^2)^{\frac{1}{2}}+|a|\}^{\frac{1}{2}}}{1-(|a|^2+b^2)^{\frac{1}{2}}}\right]. \tag{6}$$

In terms of the microwave frequency ω, the electron cyclotron frequency ω_c, the collision frequency for momentum transfer ν, and the plasma frequency ω_p, the real part of the dielectric constant is

$$a = 1+\frac{\omega_p^2}{\omega}\left\{\frac{(\omega+\omega_c)(\nu^2+\omega_c^2-\omega^2)-2\nu^2\omega}{(\nu^2+\omega_c^2-\omega^2)^2+4\omega^2\nu^2}\right\}, \tag{7}$$

which, as $\nu \to 0$, approaches

$$1+\frac{\omega_p^2}{\omega(\omega_c-\omega)}. \tag{8}$$

The imaginary part is

$$b = \frac{\omega_p^2\nu}{\omega}\left\{\frac{\nu^2+\omega_c^2-\omega^2+2\omega(\omega+\omega_c)}{(\nu^2+\omega_c^2-\omega^2)^2+4\nu^2\omega^2}\right\}, \tag{9}$$

and this, as $\nu \to 0$, approaches

$$\frac{\omega_p^2\nu}{\omega(\omega-\omega_c)^2}. \tag{10}$$

These expressions describe the RHCP wave when ω_c is taken as positive and the LHCP wave when ω_c is taken as negative. Thus, the expressions (1) and (2) describe the RHCP wave for all densities (i.e. all ω_p) when $\omega_c > \omega$, and for densities such that $\omega_p^2 < \omega(\omega-\omega_c)$ when $\omega_c < \omega$; they describe the LHCP wave in the region $\omega_p^2 < \omega(\omega+\omega_c)$. In terms of the plasma electron density n, the magnetic induction field B, and the electronic charge e and mass m, the plasma and cyclotron frequencies are given by

$$\omega_p^2 = \frac{ne^2}{\epsilon_0 m}; \qquad \omega_c = \frac{eB}{m}.$$

For convenience, the electron density is expressed in terms of the critical "cutoff" value

$$n_c = \epsilon_0 m\omega^2/e^2.$$

Our calculations avoid the near vicinity of cyclotron resonance, for here the nonlinear terms of the Boltzmann equation, which together with Maxwell's equations form the basis for the derivation of (7) and (9), present severe analytic difficulties.

From the relations (3)–(10) it is clear that the RHCP and LHCP waves will be reflected differently in both amplitude and phase.

If both rotating components are present in the incident wave, as for instance in the case of linear polarization, the reflected wave will, in general, be elliptically polarized. This is the magneto-microwave Kerr effect. Physically, the influence of the plasma on the rotating waves is the same as that involved in the Faraday effect, but the rotation and damping here arise within the skin depth. The effect is additive for penetration into the skin and emergence, because the RHCP wave rotates consistently in the same sense as the orbiting plasma electrons and the LHCP wave rotates consistently in the opposite direction.

For the case of an incident wave that is linearly polarized we consider separately its RHCP and LHCP components. In compounding these waves after reflection to construct the component with linear polarization in the same plane as the incident wave (which we call the "vertical" polarization), we add two travelling waves $|r_\mathrm{R}|\exp \mathrm{j}(\omega t+\theta_\mathrm{R}+\beta z)$ and $|r_\mathrm{L}|\exp \mathrm{j}(\omega t+\theta_\mathrm{L}+\beta z)$, where z is the direction of propagation which is collinear with the direction of the magnetic induction field B. The component linearly polarized in a direction orthogonal to this (the "horizontal" direction) is found from the superposition of two similar reflected waves but with arguments $\omega t+\theta_\mathrm{R}+\frac{1}{2}\pi+\beta z$ and $\omega t+\theta_\mathrm{L}-\frac{1}{2}\pi+\beta z$.

Experimentally, these orthogonally polarized components of the elliptically polarized reflected wave can be separately monitored with square-law detectors that display power in the two polarizations. It is easily shown that the output signals from such detectors are

$$P_\mathrm{V} = A\{|r_\mathrm{R}|^2+|r_\mathrm{L}|^2+2\,|r_\mathrm{R}|\,|r_\mathrm{L}|\cos(\theta_\mathrm{L}-\theta_\mathrm{R})\} \tag{11}$$

for the vertically polarized wave and

$$P_\mathrm{H} = A\{|r_\mathrm{R}|^2+|r_\mathrm{L}|^2-2\,|r_\mathrm{R}|\,|r_\mathrm{L}|\cos(\theta_\mathrm{L}-\theta_\mathrm{R})\} \tag{12}$$

for the horizontally polarized wave. It is convenient to normalize these expressions by choosing the constant A to be $\frac{1}{4}$, so that perfect reflection would give unity for the reflected power with vertical polarization. The determination of absolute values of electron density from these power signals, through equations (11) or (12), requires that the signals be accurately referred to the value obtained with a perfect reflector, a requirement that presents experimental difficulties. Nevertheless, they are sensitive to electron density throughout much of the range of present laboratory interest and can readily provide qualitative information of plasma density behaviour. If a single reliable measurement of electron density can be made by some other means (e.g. by microwave interferometry or the Stark broadening of spectral lines) these power signals can measure relative densities over a considerable range beyond this.

However, the ratio of the two orthogonal signals is independent of the arbitrary constant and can thus yield absolute measurements. As we shall see from the computed curves (see later, Fig. 3), this ratio is a very sensitive function of electron density. Further, it is capable of giving an indication of the collision frequency.

III. Computations

Microwave equipment has been devised which is capable of separately detecting the right-hand and left-hand circularly polarized waves or of monitoring two orthogonal linearly polarized components (Harvey 1963). With probe techniques (Takeda and Tsukishima 1963) one can separately observe the phase and amplitude of each wave.

Relevant to such experimental methods are the theoretical dependences on plasma parameters of the primary quantities $|r_R|$, $|r_L|$, θ_R, θ_L as well as the functions (11) and (12) and any other measurable combinations with marked dependence on electron density or collision frequency. The behaviour of the amplitudes and phases of the RHCP and LHCP waves is plotted in Figures 1(*a*) and 1(*b*). The effect of reflection for an incident linearly polarized wave is shown in Figure 2, which shows the magnitudes of the reflected components with both vertical and horizontal polarizations. In Figure 3 the ratio of the power in each of these two linearly polarized component waves is plotted.

IV. Discussion

It is of interest to note some of the salient general properties of the various amplitudes and phases of the reflected circularly polarized waves. From Figures 1(*a*) and 1(*b*), or quite readily from equations (3)–(10) in the case $\nu = 0$, a similarity is apparent in the density dependence of the amplitudes and phases respectively of the LHCP (for all ω and ω_c) and RHCP (for $\omega_c < \omega$) waves. Over most of the density range plotted the dielectric constant has positive real part for both of these waves, and they are therefore both described by equations (3) and (4). In Table 1 we summarize the most prominent properties of the circularly polarized waves.

From a plasma diagnostic point of view there are some particularly relevant features to be noted. The phase shift θ_L of the LHCP wave is sensitive to high electron densities over a wide range and for a wide variety of wave frequencies and magnetic induction fields. For sufficiently large magnetic induction fields the RHCP wave is never "cut off" (i.e. totally reflected), and the reflected amplitude is strongly dependent on electron densities over the wide range from below 10^{12} cm^{-3} to above 10^{16} cm^{-3}.

If the microwave reflection is required to indicate collision frequency, it is clear that this will be best performed at the two densities corresponding to $\omega_p^2 = \omega(\omega+\omega_c)$ and $\omega_p^2 = \omega(\omega-\omega_c)$, where most of the wave properties are affected by collisions. Since the important parameter here is ν/ω the choice of microwave frequency is important.

The cutoff points for both the RHCP (when $\omega_c < \omega$) and LHCP waves are sharp and can provide a useful measure of two discrete electron densities, that for the LHCP wave being at a density higher by a factor $1+\omega_c/\omega$ than the highest density (n_c) normally accessible to microwave interferometry when transmission of the ordinary wave (that travelling across the magnetic induction field with its

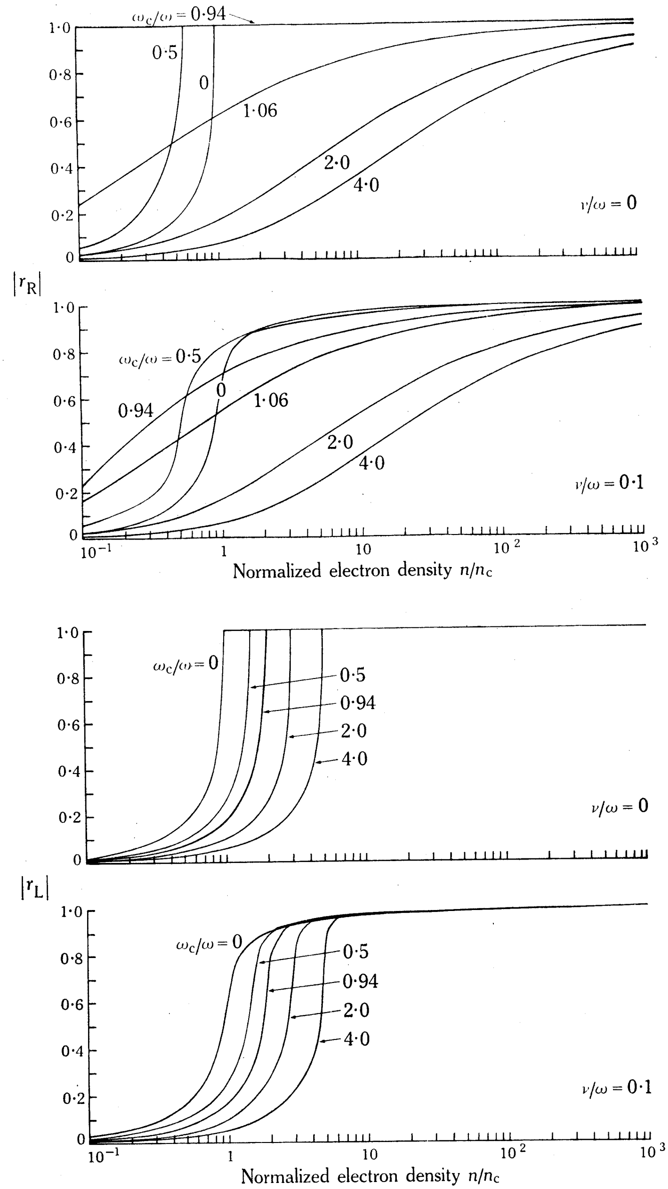

Fig. 1(a).—The magnitudes $|r_R|$ and $|r_L|$ of the reflection coefficients of the RHCP and LHCP waves, plotted against plasma electron density (normalized) with the electron cyclotron frequency and wave and collision frequencies (ω_c, ω, and ν respectively) as parameters. The reflecting surface has a step-function density profile, and the magnetic field and wave propagation direction are normal to the surface.

E vector parallel to that field) is used. For the ordinary wave, to which our curves with $\omega_c/\omega = 0$ are directly applicable, the abruptness of the reflection at cutoff has proved to be of considerable use in laboratory experimentation (Robinson and Sharp 1963).

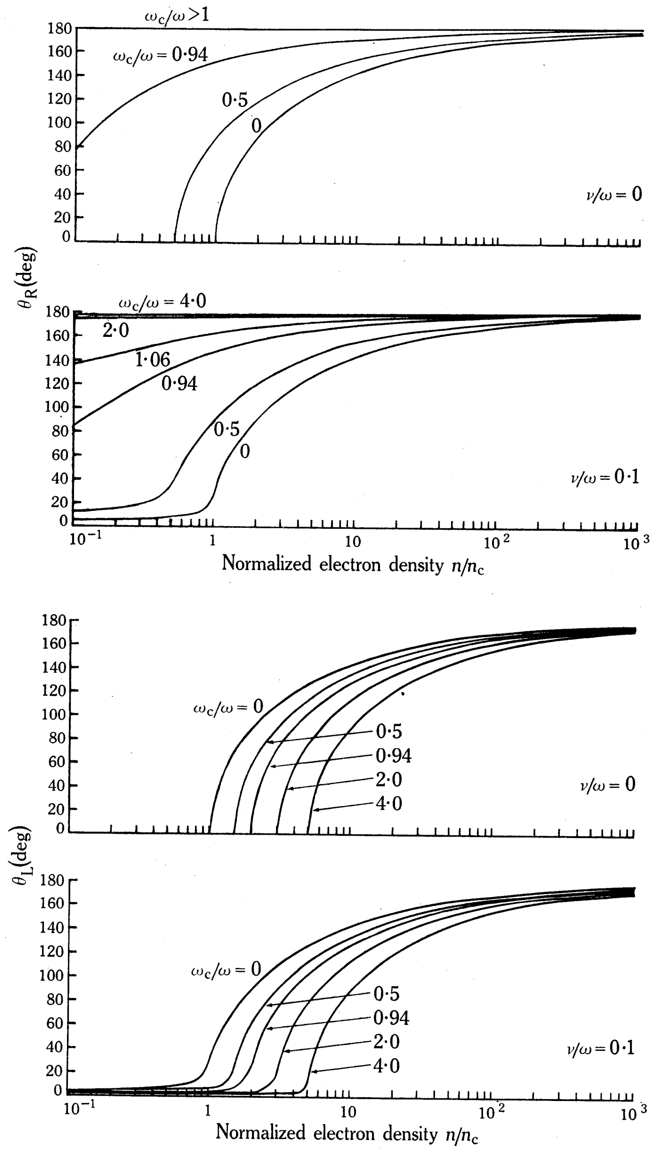

Fig. 1(*b*).—The arguments θ_R and θ_L of the reflection coefficients of the RHCP and LHCP waves, plotted against plasma electron density (normalized) with the electron cyclotron frequency and wave and collision frequencies (ω_c, ω, and ν respectively) as parameters. The reflecting surface has a step-function density profile, and the magnetic field and wave propagation direction are normal to the surface.

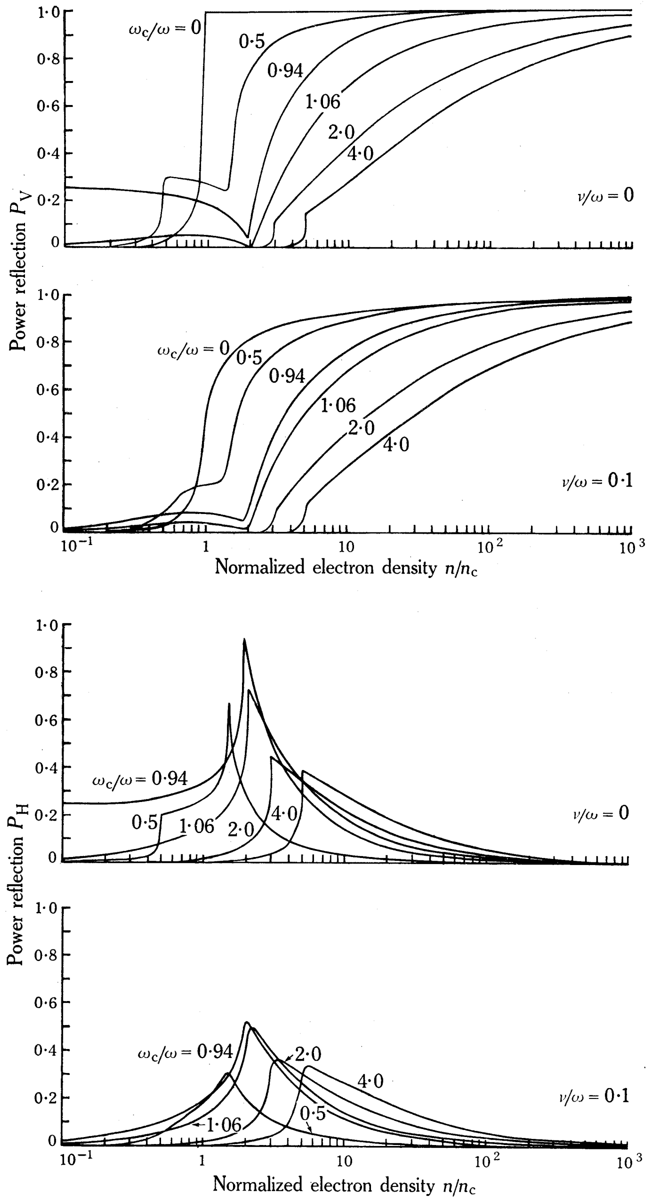

Fig. 2.—The theoretical output currents of square-law detectors monitoring microwave signals reflected from a plasma boundary with (*upper*) the same linear polarization as the incident wave ("vertical" polarization) and with (*lower*) the orthogonal polarization ("horizontal" polarization), plotted against plasma electron density (normalized) with the electron cyclotron frequency and wave and collision frequencies (ω_c, ω, ν) as parameters. The reflecting surface has a step-function density profile, and the magnetic field and wave propagation direction are normal to the surface.

The magneto-Kerr effect, as observed through the two orthogonal linearly polarized reflected waves, has the merit that the horizontally polarized component wave is not only sensitive to electron density and high collision frequencies but

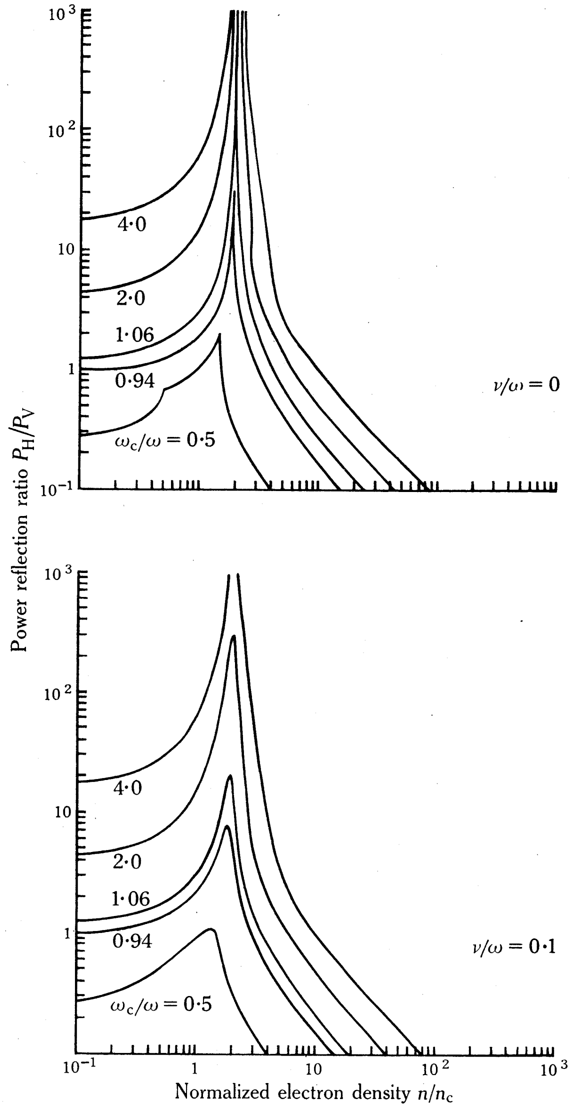

Fig. 3.—The ratio P_H/P_V of power in the two orthogonal reflected wave components of Figure 2.

has a marked peak when $\omega_p^2 = \omega(\omega+\omega_c)$. This peak has such a well-defined shape that it is readily recognized in experimental records and gives a precise reference density point $n_c(1+\omega_c/\omega)$. The marked dependence of the height of the peak on collision frequency can provide a good indication of the value of this parameter.

Most importantly, and as we can see from equations (11) and (12), the ratio of the power with horizontal polarization to that with vertical polarization is independent of the arbitrary constant A and so can yield absolute measurements of electron density. As we see from Figure 3, this ratio is highly sensitive to electron density, and the magnitude of the peak at $\omega_p^2 = \omega(\omega+\omega_c)$ is significantly dependent on collision frequency.

TABLE 1

PROPERTIES OF REFLECTED CIRCULARLY POLARIZED WAVES

Wave Property	Condition	Dependence on Electron Density	Dependence on Collision Frequency
Amplitude of RHCP wave, $\lvert r_R \rvert$	$\omega_c/\omega < 1$ $\omega_p^2 > \omega(\omega-\omega_c)$	Total reflection over density range	ν effective when $\omega_p^2 \approx \omega(\omega-\omega_c)$
	$\omega_c/\omega > 1$	Sensitive function over large density range	—
Amplitude of LHCP wave, $\lvert r_L \rvert$	$\omega_p^2 > \omega(\omega+\omega_c)$	Total reflection over large density range	ν effective when $\omega_p^2 \approx \omega(\omega+\omega_c)$
Phase of RHCP wave, θ_R	$\omega_c/\omega < 1$ $\omega_p^2 > \omega(\omega-\omega_c)$	Sensitive function over large density range	ν effective when $\omega_p^2 \approx \omega(\omega-\omega_c)$
	$\omega_c/\omega > 1$	—	—
Phase of LHCP wave, θ_L	$\omega_p^2 > \omega(\omega+\omega_c)$	Sensitive function over large density range	ν effective when $\omega_p^2 \approx \omega(\omega+\omega_c)$

Associated with the small distance of plasma–wave interaction for reflected waves (the skin depth) there is the advantage over transmitted waves that they are less attenuated. Faraday rotation experiments usually involve transmission over quite long paths, which, for moderate collision frequencies, are usually heavily attenuated. For this reason, this effect has found application only at densities far below those accessible to reflection methods. But, of course, the plasma geometry required for the application of transmission is far less particular than that demanded for reflection studies.

It is of interest to note some very recent developments in semiconductor physics, running parallel to those here discussed in plasma physics, where the free-carrier magneto-microwave Kerr effect has been successfully used to circumvent the problem of transmission loss in high conductivity semiconductors associated with the Faraday effect (Brodwin and Vernon 1965). These studies investigate reflection of the TE_{11} propagation mode in a circular waveguide and, together with the considerable literature concerned with guided-wave propagation in gyromagnetic media (see, for instance, Suhl and Walker 1954), have considerable interest for the study of the magneto-microwave Kerr effect for circular waveguide plasma probes.

V. Effect of Density Gradients

It is natural to examine the importance to the preceding discussion of the assumption of a step-function plasma boundary. To answer this question, we consider a plane wave interacting with a semi-infinite plane plasma with an increasing density profile and solve the wave equation for the fields in the inhomogeneous region. By matching these fields at the plasma boundary to fields in the free-space region, where we suppose incident and reflected plane waves to be present, we can calculate the reflection coefficient.

The electric vector in the plasma satisfies the wave equation

$$\nabla\times\nabla\times\mathbf{E}+k_0^2\,\boldsymbol{\varepsilon}\,\mathbf{E}=0, \tag{13}$$

where $k_0 = \omega/c$ and

$$\boldsymbol{\varepsilon}\,\mathbf{E}=\begin{pmatrix}\epsilon_{xx} & \epsilon_{xy} & 0\\ \epsilon_{yx} & \epsilon_{yy} & 0\\ 0 & 0 & \epsilon_{zz}\end{pmatrix}\begin{pmatrix}E_x\\ E_y\\ 0\end{pmatrix},$$

the Cartesian elements of the dielectric-constant tensor being

$$\epsilon_{xx}=\quad\epsilon_{yy}=1+\frac{\omega_{\mathrm{p}}^2}{\omega}\left\{\frac{\omega-\mathrm{j}\nu}{(\mathrm{j}\omega+\nu)^2+\omega_{\mathrm{c}}^2}\right\},$$

$$\epsilon_{xy}=-\epsilon_{yx}=\frac{\omega_{\mathrm{p}}^2}{\omega}\left\{\frac{\mathrm{j}\omega_{\mathrm{c}}}{(\mathrm{j}\omega+\nu)^2+\omega_{\mathrm{c}}^2}\right\}.$$

If we write the Cartesian components of the electric field in terms of the RHCP and LHCP components $E_{\mathrm{R,L}} = E_x \pm \mathrm{j}E_y$ and substitute in (13) for E_x and E_y, we find that the circularly polarized fields obey the wave equation

$$\frac{\mathrm{d}^2E_{\mathrm{R}}}{\mathrm{d}z^2}+k_0^2\epsilon_{\mathrm{R}}E_{\mathrm{R}}=0,\qquad \frac{\mathrm{d}^2E_{\mathrm{L}}}{\mathrm{d}z^2}+k_0^2\epsilon_{\mathrm{L}}E_{\mathrm{L}}=0, \tag{14}$$

where $\epsilon_{\mathrm{R}} = \epsilon_{xx}-\mathrm{j}\epsilon_{xy}$ and $\epsilon_{\mathrm{L}} = \epsilon_{xx}+\mathrm{j}\epsilon_{xy}$ are as given in equation (1).

Differential equations of the form (14) have been studied with a variety of dependences of ϵ upon z (Morse and Feshbach 1953; Albini and Jahn 1961; Budden 1961; Wait 1962; Yen 1964). Let up suppose (with Yen) that the region of inhomogeneous plasma begins at $z = 0$ and that for $z > 0$ the electron density varies as

$$n=n_{\max}\{1-\exp(-\gamma\,2\pi z/\lambda)\}, \tag{15}$$

γ being a constant specifying the steepness of the density profile and λ the free-space wavelength. The effective complex dielectric constant of the plasma can then be written

$$\epsilon_{\mathrm{R,L}}=1-K_{\mathrm{R,L}}\{1-\exp(-\gamma\,2\pi z/\lambda)\}, \tag{16}$$

where

$$K_{\mathrm{R,L}} = \frac{(\omega_{\mathrm{p}}^2)_{\max}}{\omega}\left[\frac{(\omega\pm\omega_{\mathrm{c}})(\omega^2-\omega_{\mathrm{c}}^2-\nu^2)+2\nu^2\omega+\mathrm{j}\nu\{(\omega\pm\omega_{\mathrm{c}})^2+\nu^2\}}{(\omega^2-\omega_{\mathrm{c}}^2-\nu^2)^2+4\nu^2\omega^2}\right]. \tag{17}$$

In these expressions $n_{\max}$ and $(\omega_{\mathrm{p}})_{\max}$ stand for the electron density and plasma frequency respectively at $z = \infty$.

In solving the differential equation (14) with $\epsilon_{\mathrm{R,L}}$ varying with z as in (16), let us omit the subscripts R,L with the understanding that the derived results apply to both the RHCP and LHCP waves when appropriate substitutions are made from (1) but, of course, with ω_{p} replaced by $(\omega_{\mathrm{p}})_{\max}$. In the wave equation

$$\frac{\mathrm{d}^2E}{\mathrm{d}z^2}+k_0^2\epsilon E = 0,$$

the change of variable from z to ξ by the transformation

$$\xi = (2K^{\frac{1}{2}}/\gamma)\exp(-\gamma\pi z/\lambda) \tag{18}$$

reduces the equation to the form

$$\xi^2\frac{\mathrm{d}^2E}{\mathrm{d}\xi^2}+\xi\frac{\mathrm{d}E}{\mathrm{d}\xi}+(\xi^2-\tau^2)E = 0, \tag{19}$$

where

$$\tau = \mathrm{j}(2/\gamma)(1-K)^{\frac{1}{2}} = \mathrm{j}(2/\gamma)\epsilon_{\max}^{\frac{1}{2}}. \tag{20}$$

This is Bessel's equation of (complex) order τ and (complex) argument ξ (Watson 1952). The solutions are

$$E = C\,\mathrm{J}_\tau(\xi)+D\,\mathrm{J}_{-\tau}(\xi), \tag{21}$$

with C and D constants and the Bessel functions defined by the power-series expansions

$$\mathrm{J}_\tau(\xi) = \left(\frac{\xi}{2}\right)^\tau\left\{\frac{1}{\Gamma(\tau+1)}-\frac{(\frac{1}{2}\xi)^2}{\Gamma(\tau+2)}+\frac{(\frac{1}{2}\xi)^4}{2\,\Gamma(\tau+3)}\cdots\right\}, \tag{22}$$

$$\mathrm{J}_{-\tau}(\xi) = \left(\frac{\xi}{2}\right)^{-\tau}\left\{\frac{1}{\Gamma(-\tau+1)}-\frac{(\frac{1}{2}\xi)^2}{\Gamma(-\tau+3)}+\frac{(\frac{1}{2}\xi)^4}{2\,\Gamma(-\tau+3)}\cdots\right\}. \tag{23}$$

To decide whether these solutions are acceptable, consider their behaviour as z approaches infinity. Observe that in this limit the second terms inside the bracketed power series vary as $\exp(-\gamma\,2\pi z/\lambda)$, which tends to zero as z approaches infinity, and likewise for subsequent terms. For large z, then,

$$\mathrm{J}_\tau(\xi) \sim \exp(-\gamma\pi\tau z/\lambda) = \exp\{-(2\pi/\lambda)\,\mathrm{j}\epsilon_{\max}^{\frac{1}{2}}z\},$$

clearly representing a wave travelling in the $+z$ direction. Similarly,

$$\mathrm{J}_{-\tau}(\xi) \sim \exp(\gamma\pi\tau z/\lambda) = \exp\{(2\pi/\lambda)\,\mathrm{j}\epsilon_{\max}^{\frac{1}{2}}z\},$$

representing a wave travelling in the $-z$ direction. Now, we can write

$$\epsilon_{\max}^{\frac{1}{2}} = \alpha_0-\mathrm{j}\beta_0. \tag{24}$$

If we choose α_0 and β_0 both positive (to ensure that the wave $\exp \mathrm{j}(\omega t - k_0 \epsilon^{\frac{1}{2}} z)$ travelling into the plasma is attenuated), then $\mathrm{J}_{-\tau}(\xi)$ represents a wave that grows infinitely as $z \to \infty$. It is therefore a physically unrealistic solution.

The electric field in the plasma is, therefore,

$$E = C\,\mathrm{J}_\tau(\xi). \tag{25}$$

The reflection coefficient can now be determined by supposing in the free-space region $z < 0$ an incident plane transverse wave $\exp \mathrm{j}(\omega t - k_0 z)$ and a reflected wave $R \exp \mathrm{j}(\omega t + k_0 z)$ and by matching these fields to the field $E = C\,\mathrm{J}_\tau(\xi)$ at $z = 0$. When $z = 0$, $\xi = 2K^{\frac{1}{2}}/\gamma$, and the boundary conditions that E and $\partial E/\partial z$ be continuous give

$$R + 1 = C\,\mathrm{J}_\tau(2K^{\frac{1}{2}}/\gamma) \tag{26}$$

and

$$R - 1 = \mathrm{j}\,CK^{\frac{1}{2}}\,\mathrm{J}'_\tau(2K^{\frac{1}{2}}/\gamma), \tag{27}$$

the dash indicating the derivative with respect to ξ. Whence,

$$R = \left[1 + \mathrm{j}K^{\frac{1}{2}}\left\{\frac{\mathrm{J}'_\tau(2K^{\frac{1}{2}}/\gamma)}{\mathrm{J}_\tau(2K^{\frac{1}{2}}/\gamma)}\right\}\right] \times \left[1 - \mathrm{j}K^{\frac{1}{2}}\left\{\frac{\mathrm{J}'_\tau(2K^{\frac{1}{2}}/\gamma)}{\mathrm{J}_\tau(2K^{\frac{1}{2}}/\gamma)}\right\}\right]^{-1}. \tag{28}$$

Using now the recurrence relationships between Bessel functions (see Watson)

$$\xi\,\mathrm{J}'_\tau(\xi) - \tau\,\mathrm{J}_\tau(\xi) = -\xi\,\mathrm{J}_{\tau+1}(\xi),$$

$$\mathrm{J}_\tau(\xi) + \mathrm{J}_{\tau+2}(\xi) = \{2(\tau+1)/\xi\}\,\mathrm{J}_{\tau+1}(\xi),$$

we can put equation (28) into the form

$$R = \left(\frac{1-\epsilon_{\max}^{\frac{1}{2}}}{1+\epsilon_{\max}^{\frac{1}{2}}}\right) F, \tag{29}$$

where

$$F = \left[1 - \frac{\mathrm{j}(1+\epsilon_{\max}^{\frac{1}{2}})}{\gamma(\tau+1)}\left\{1 + \frac{\mathrm{J}_{\tau+2}(2K^{\frac{1}{2}}/\gamma)}{\mathrm{J}_\tau(2K^{\frac{1}{2}}/\gamma)}\right\}\right] \times \left[1 + \frac{\mathrm{j}(1-\epsilon_{\max}^{\frac{1}{2}})}{\gamma(\tau+1)}\left\{1 + \frac{\mathrm{J}_{\tau+2}(2K^{\frac{1}{2}}/\gamma)}{\mathrm{J}_\tau(2K^{\frac{1}{2}}/\gamma)}\right\}\right]^{-1}. \tag{30}$$

The complex factor F can be written as $B\,\mathrm{e}^{\mathrm{j}\delta}$, where B is the factor by which the magnitude of the reflection coefficient is reduced below that from a step-function profile and δ is the increase in phase produced by the exponential plasma density profile. Polynomial expressions for B and δ can be obtained by writing

$$1 + \frac{\mathrm{J}_{\tau+2}(2K^{\frac{1}{2}}/\gamma)}{\mathrm{J}_\tau(2K^{\frac{1}{2}}/\gamma)} = p + \mathrm{j}q \tag{31}$$

and substituting for $\epsilon_{\max}$ and τ from (24) and (20). This gives

$$B = \left[\frac{\{\gamma + 2\beta_0 - p\beta_0 + q(\alpha_0+1)\}^2 + \{2\alpha_0 - p(\alpha_0+1) - q\beta_0\}^2}{\{\gamma + 2\beta_0 - p\beta_0 + q(\alpha_0-1)\}^2 + \{2\alpha_0 - p(\alpha_0-1) - q\beta_0\}^2}\right]^{\frac{1}{2}}, \tag{32}$$

which approaches

$$\left\{\frac{(\gamma+\beta_0)^2 + (\alpha_0-1)^2}{(\gamma+\beta_0)^2 + (\alpha_0+1)^2}\right\}^{\frac{1}{2}} \tag{33}$$

when $p \to 1$ and $q \to 0$, i.e. when $J_{\tau+2}(2K^{\frac{1}{2}}/\gamma)/J_\tau(2K^{\frac{1}{2}}/\gamma)$ is negligibly small, and

$$\delta = \tan^{-1}\left\{\frac{2\alpha_0 - p(\alpha_0+1) - q\beta_0}{\gamma + 2\beta_0 - p\beta_0 + q(\alpha_0+1)}\right\} - \tan^{-1}\left\{\frac{2\alpha_0 - p(\alpha_0-1) - q\beta_0}{\gamma + 2\beta_0 - p\beta_0 + q(\alpha_0-1)}\right\}, \tag{34}$$

which approaches

$$\tan^{-1}\left(\frac{\alpha_0-1}{\gamma+\beta_0}\right) - \tan^{-1}\left(\frac{\alpha_0+1}{\gamma+\beta_0}\right) \tag{35}$$

when $p \to 1$ and $q \to 0$.

In the limit $\gamma \to \infty$ the profile becomes a step function, and, as required, $B = 1$ and $\delta = 0$, i.e. $F = 1$ and

$$R = \frac{1-\epsilon_{\max}^{\frac{1}{2}}}{1+\epsilon_{\max}^{\frac{1}{2}}}.$$

The expressions (32)–(35) involve the quantities α_0 and β_0 given by (2) and (24):

$$\left.\begin{aligned}\alpha_0 &= \left\{\frac{(a^2+b^2)^{\frac{1}{2}}+a}{2}\right\}^{\frac{1}{2}},\\ \beta_0 &= \left\{\frac{(a^2+b^2)^{\frac{1}{2}}-a}{2}\right\}^{\frac{1}{2}}.\end{aligned}\right\} \tag{36}$$

For a collisionless plasma, $a > 0$ for the RHCP wave when $\omega_c > \omega$ and for the LHCP wave when $\omega_p^2 < \omega(\omega+\omega_c)$, while $a < 0$ for the RHCP wave when $\omega_c < \omega$ and $\omega_p^2 > \omega(\omega-\omega_c)$ and for the LHCP wave when $\omega_p^2 > \omega(\omega+\omega_c)$.

Tables of Bessel functions with complex argument and complex order are not available, but one can calculate the p's and q's involved in (32) and (34) from the series expansion (22). From (22) and (31) we obtain

$$\begin{aligned}p+\mathrm{j}q &\\ = 1 + \frac{K}{\gamma^2}&\left\{\frac{1}{(\tau+2)(\tau+1)} - \frac{K}{\gamma^2}\frac{1}{(\tau+3)(\tau+2)(\tau+1)} + \frac{K^2}{2\gamma^4}\frac{1}{(\tau+4)(\tau+3)(\tau+2)(\tau+1)}\cdots\right\}\\ &\times\left\{1 - \frac{K}{\gamma^2}\frac{1}{(\tau+1)} + \frac{K^2}{2\gamma^4}\frac{1}{(\tau+2)(\tau+1)}\cdots\right\}^{-1}.\end{aligned} \tag{37}$$

We have computed B and δ from (32) and (34), for both the RHCP and LHCP waves, as functions of electron density with magnetic field and collision frequency as parameters. Representative curves are plotted in Figures 4(*a*) and 4(*b*). Here the steepness of the density profile has been specified by choosing $\gamma = 10$, for which value the density rises to 96% of its maximum downstream value in 0·05 free-space wavelengths.

The most marked feature of these curves is that the development of a density gradient can substantially change the phase angles of both the reflected RHCP and LHCP waves. Thus, although the phase angles, particularly that of the LHCP wave, are sensitive functions of density for a wide variety of plasma conditions, their interpretation in terms of electron densities is susceptible to significant gradient-introduced errors.

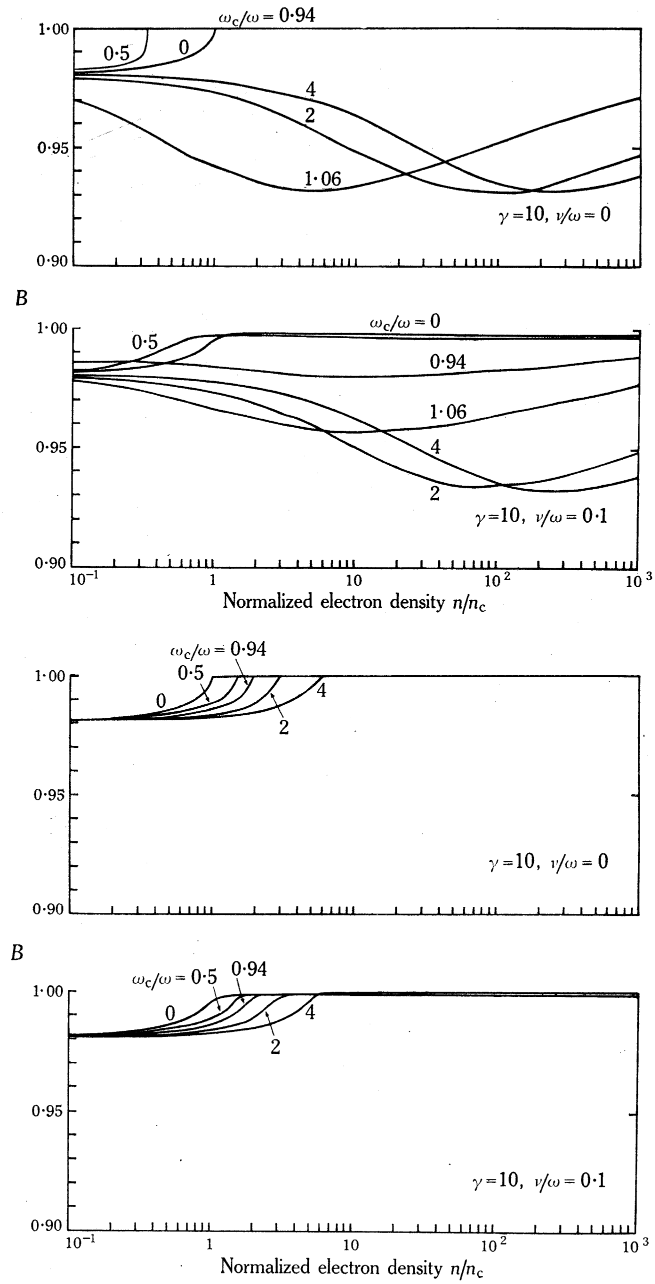

Fig. 4(a).—The factors B by which the magnitudes of the RHCP (*upper*) and LHCP waves (*lower*) are reduced, at reflection from an exponential plasma boundary specified by γ, below that from a step-function boundary, plotted against plasma electron density (normalized) with the electron cyclotron frequency and wave and collision frequencies (ω_c, ω, ν) as parameters. The magnetic field and wave propagation direction are normal to the plane vacuum–plasma boundary.

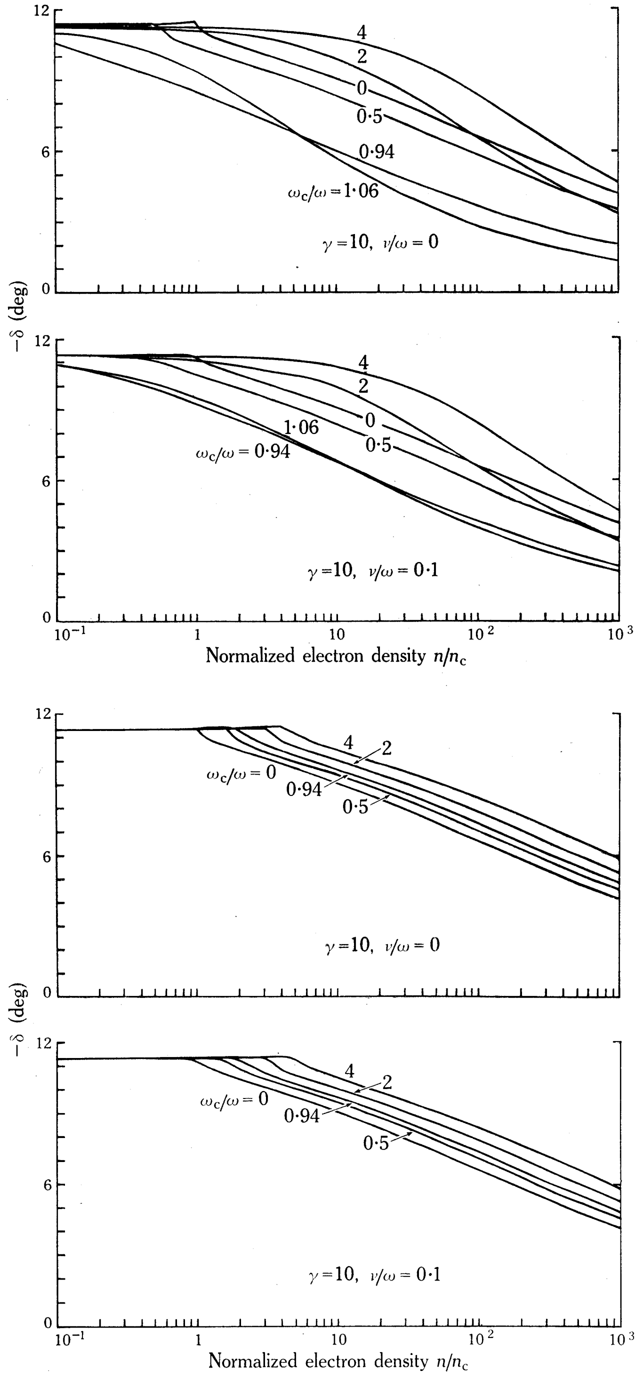

Fig. 4(*b*).—The angles δ by which the phases of the RHCP (*upper*) and LHCP waves (*lower*) are changed, at reflection from an exponential plasma boundary specified by γ, below that from a step-function boundary, plotted against plasma electron density (normalized) with the electron cyclotron frequency and wave and collision frequencies (ω_c, ω, ν) as parameters. The magnetic field and wave propagation direction are normal to the plane vacuum–plasma boundary.

The amplitude of the LHCP wave is affected to a relatively minor extent by the development of a gradient, and that of the RHCP wave can be decreased by up to 7% as the gradient tends to "match in" this wave.

In Table 2 we summarize the effect of a gradient on the power in the two orthogonal linearly polarized reflections for some chosen values of the plasma density and other parameters. From these values one can find the error in the ratio P_H/P_V that arises from assuming a step-function interface when the profile is actually an exponential specified by $\gamma = 10$. From the curves of Figure 3, then, the error in estimated densities can be found. For the case $\omega_c/\omega = 2$ in Table 2 the error is only a few percent, except for $n/n_c = 100$ when it is about 7%. For $\omega_c/\omega = 0 \cdot 94$ the three lower densities have errors of only a few percent, but those for $n/n_c = 10$ and 100 have errors of 15% and 96% respectively. The generally small effect of

TABLE 2

EFFECT OF ELECTRON DENSITY GRADIENTS ON REFLECTED POWER

n/n_c	ω_c/ω	ν/ω	γ	Decrease of Vertically Polarized Power P_V (%)	Decrease of Horizontally Polarized Power P_H (%)
0·1	0·94	0·1	10	3·0	2·9
1				5·0	2·4
3				5·9	−2·8*
10				3·9	−11·7
100				2·5	−53·9
10	2	0·1	10	3·1	0·6
100				6·2	−21·9

* Negative sign means that the power increases with the development of the gradient.

the gradient on P_V and P_H can be anticipated from the curves of Figure 4(*b*). Although θ_L and θ_R can both decrease by as much as 11° it is their difference that appears in the expressions (11) and (12) for P_V and P_H, and this difference undergoes little change when the gradient develops.

Because $\theta_L - \theta_R$ is little affected by a gradient but is a sensitive function of electron density, it appears to offer a valuable means for the measurement of surface electron densities. Further, if the relative phase shift is found from measurements of θ_L and θ_R separately, then, from the density obtained from their difference, either phase shift can be used to give a measure of the gradient. When the interface is a step function, $\theta_L - \theta_R$, θ_R, and θ_L will, of course, all indicate the same density, but in other situations the extent to which they yield different results is a measure of the gradient.

We have found for $\gamma = 5$ that $\theta_L - \theta_R$ is still little altered, but for $\gamma = 2$ (for which the density reaches 96% of its peak value in 0·25 free-space wavelengths) the gradient does affect $\theta_L - \theta_R$. For a gradual profile, like $\gamma = 2$, one can still obtain a measure of both density and gradient as indicated above, provided iterative procedures are used to obtain the final results.

VI. Acknowledgments

The author wishes to thank S. K. Chung, N. R. Heckenberg, and G. P. Rothman for computational assistance, Dr. B. H. J. McKellar for discussions, The Australian Institute of Nuclear Science and Engineering for financial support, and Professor H. Messel and Professor C. N. Watson-Munro for providing the research facilities.

VII. References

Albini, F. A., and Jahn, R. G. (1961).—*J. appl. Phys.* **32**, 75.

Brand, G. F., Chung, S. K., and Robinson, L. C. (1966).—*Nucl. Fusion* **6**(1), 41–5.

Brodwin, M. E., and Vernon, R. J. (1965).—*Phys. Rev.* **140**, A 1390.

Budden, K. G. (1961).—"Radio Waves in the Ionosphere." (Cambridge Univ. Press.)

Harvey, A. F. (1963).—"Microwave Engineering." (Academic Press: London.)

Hermansdorfer, H. (1965).—Report IPP 1/37 of Institute for Plasma Physics, Munich, June 1965.

McLane, C. K., Takeda, S., Thomas, W. E., and Thompson, R. C. (1964).—*Bull. Am. phys. Soc.* **9**, 323.

Morse, P. M., and Feshbach, H. (1953).—"Methods of Theoretical Physics." (McGraw-Hill: New York.)

Robinson, L. C. (1965).—*J. nucl. Energy* C **7**, 167.

Robinson, L. C. (1966).—*Phys. Rev.* **145**, 91–2.

Robinson, L. C., and Sharp, L. E. (1963).—*Aust. J. Phys.* **16**, 439.

Stix, T. H. (1962).—"The Theory of Plasma Waves." (McGraw-Hill: New York.)

Suhl, H., and Walker, L. R. (1954).—*Bell Syst. tech. J.* **33**, 1133.

Takeda, S., and Roux, M. (1961).—*J. phys. Soc. Japan* **16**, 95.

Takeda, S., and Tsukishima, T. (1963).—*J. phys. Soc. Japan* **18**, 426.

Tsukishima, T., and Takeda, S. (1962).—*J. appl. Phys.* **33**, 3290.

Wait, J. R. (1962).—"Electromagnetic Waves in Stratified Media." (Pergamon: Oxford.)

Watson, G. N. (1952).—"A Treatise on the Theory of Bessel Functions." (Cambridge Univ. Press.)

Yen, K. T. (1964).—*J. appl. Phys.* **35**, 290.